Electronic Supplementary Information

Efficient energy transport in constant-voltage triboelectric nanogenerator based power unit

Xinyuan Li,‡[a] Zhihao Zhao,‡[a] Yuexiao Hu,‡[ac] Yikui Gao,[ab] Lixia He,[ab] Wenyan Qiao,[ab] Baofeng Zhang,[d] Youlong Xu,[f] Zhong Lin Wang,*[abf] Jie Wang,*[abc]*

[a]*CAS Center for Excellence in Nanoscience, Beijing Key Laboratory of Micro-nano Energy and Sensor, Beijing Institute of Nanoenergy and Nanosystems, Chinese Academy of Sciences, Beijing 100083, P. R. China. E-mail: wangjie@binn.cas.cn*

[b]*School of Nanoscience and Technology, University of Chinese Academy of Sciences, Beijing 100049, P. R. China.*

[c]*Center on Nanoenergy Research, School of Physical Science and Technology, Guangxi University, Nanning, 530004, P. R. China.*

[d]*Hubei Key Laboratory of Automotive Power Train and Electronic control, School of Automotive Engineering, Hubei University of Automotive Technology, Shiyan, 442002, P. R. China.*

[e]*Electronic Materials Research Laboratory, Key Laboratory of the Ministry of Education & International Center for Dielectric Research, Xi'an Jiaotong University, Xi'an, 710049, P. R. China. E-mail: ylxu@mail.xjtu.edu.cn*

[f]*School of Materials Science and Engineering, Georgia Institute of Technology, Atlanta, GA 30332-0245, USA. E-mail: zhong.wang@mse.gatech.edu*

† Electronic Supplementary Information (ESI) available. See DOI: 10.1039/x0xx00000x

‡ These authors contributed equally to this work.

Content

Supplementary Figures:

Supplemental Tables:

Supplemental Notes:

Supplemental videos:

Supplementary Figures:

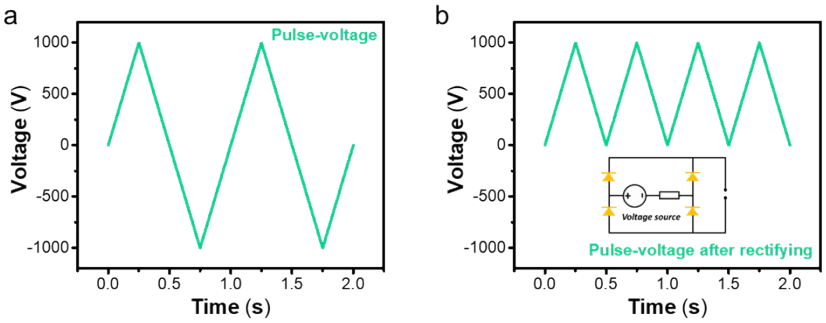

Fig. S1. Output characteristic of pulse-voltage source and pulse voltage source after rectifying. (a) Output characteristic of pulse-voltage source. (b) Output characteristic of pulse voltage source after rectifying, Inset: circuit connection. (The peak value of triangle alternating pulse-voltage source is 1000 V, its period is 1s, Diodes can reverse its opposite voltage as shown in Fig. S1b, the resistance in series with the voltage source is 10MΩ.)

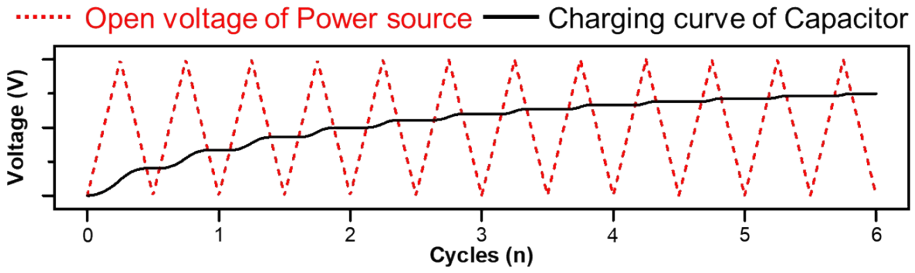

Fig. S2. Output characteristic of pulse-voltage source and charging curve of capacitor.

(The peak value of triangle alternating pulse-voltage source is 1000 V, and its period is 1s. The resistance in series with the voltage source is 10MΩ, the capacitance of the capacitor is 100 nF.)

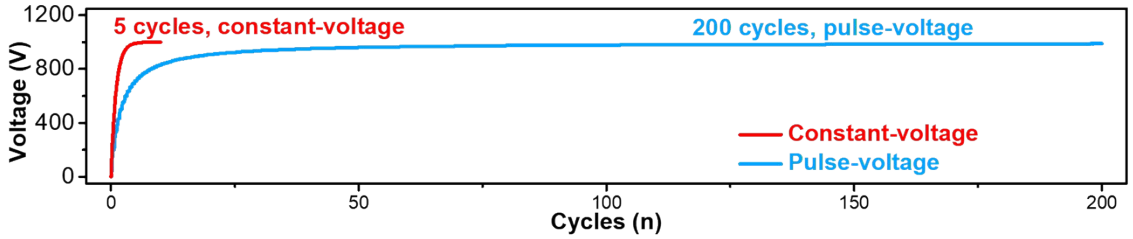

Fig. S3. The voltage curves of a capacitor charged by constant/pulse voltage sources until saturated.

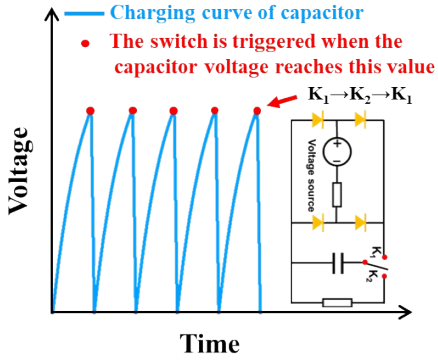

Fig. S4. The general power management strategy of TENG to obtain a continuingly stable average power.

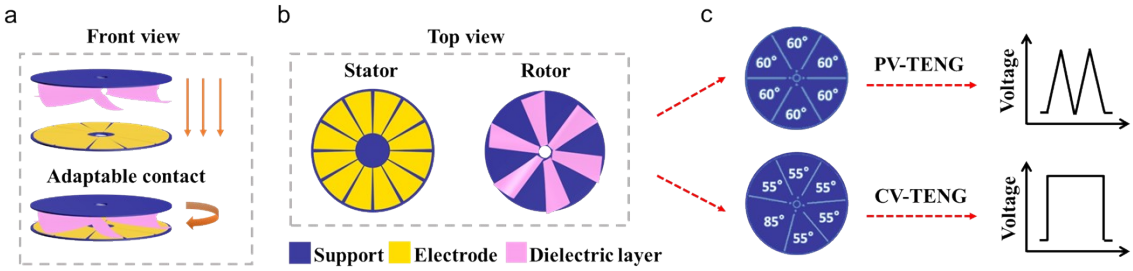

Fig. S5. The schematic diagram to fabricate CV-TENG and PV-TENG. Basic structure of CV-TENG and PV-TENG from (a) the front view and (b) the top view. (c) The slight angle difference between CV-TENG and PV-TENG. Details are visible in Note S5.

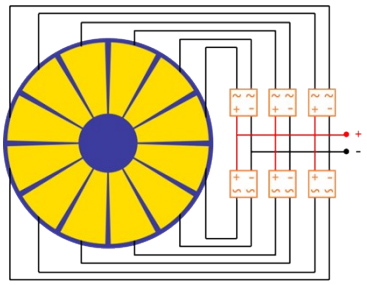

Fig. S6. The circuit connection of the TENG.

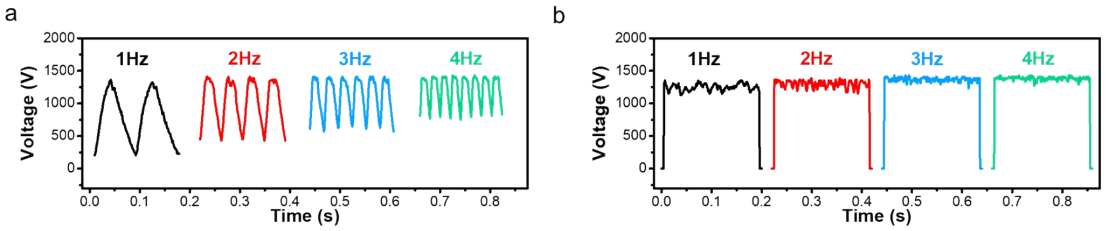

Fig. S7. Voltage performance of PV-TENG (a) and CV-TENG (b) under different frequency, respectively.

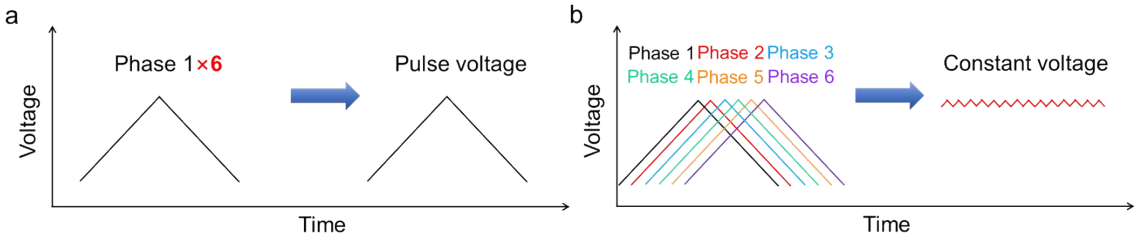

Fig. S8. Schematic voltage superposition of (a) PV-TENG and (b) CV-TENG.

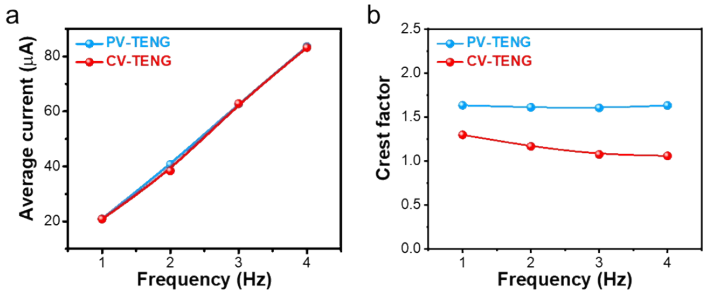

Fig. S9. The detailed current information involving average current and crest factor of PV-TENG and CV-TENG.

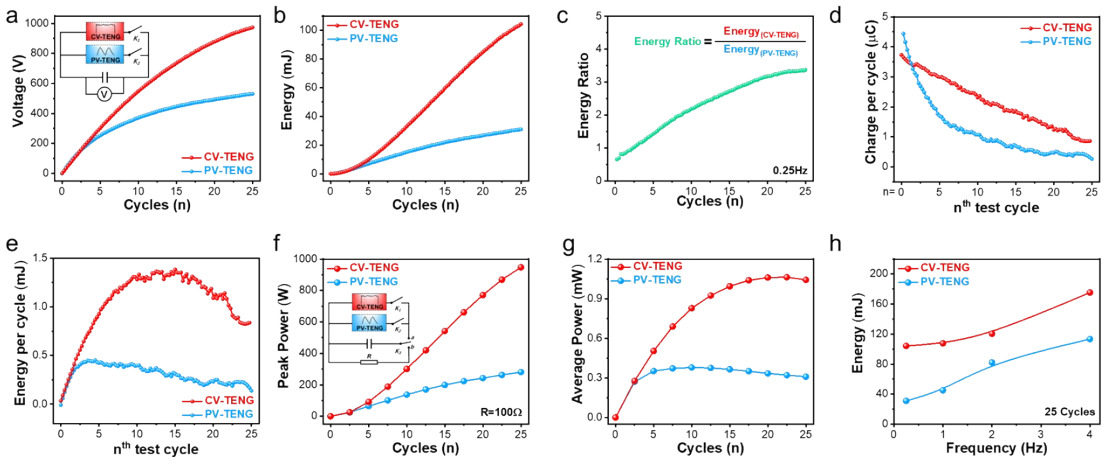

Fig. S10. The comparation between CV-TENG and PV-TENG. (a) The voltage curves of a capacitor charged by CV-TENG and PV-TENG, respectively. Inset: The circuit connection between a CV-TENG/PV-TENG and a capacitor. (b) The stored energy of a capacitor and (c) the energy ratio charged by CV-TENG and PV-TENG, respectively, versus cycles. (d) The charge per cycle flow to the capacitor versus n^{th} test cycle charged by CV-TENG/PV-TENG, respectively. (e) The energy per cycle flow to the capacitor versus n^{th} test cycle charged by CV-TENG/PV-TENG, respectively. (f) The peak power and (g) the average power of CV-TENG and PV-TENG under a capacitance load achieved by a switch. Inset of figure (f): The detailed circuit connection. (h) The stored energy of a capacitor changes versus frequency charged by CV-TENG/PV-TENG under the same charging cycles.

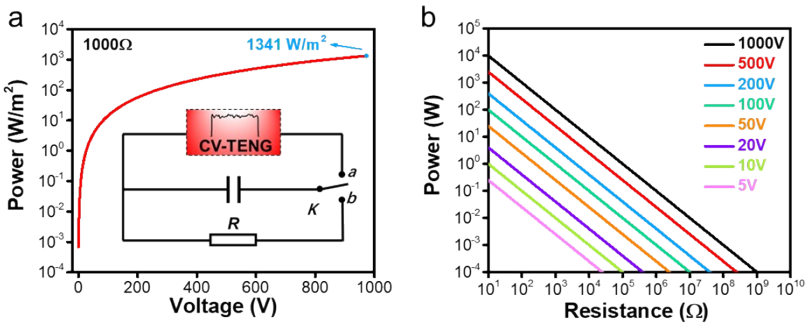

Fig. S11. Power changes versus discharging voltage and resistance load, respectively. (a) Power changes versus discharging voltage under the process of CV-TENG charging a capacitor, Inset: circuit connection. (b) Power changes versus discharging voltage and resistance load, respectively.

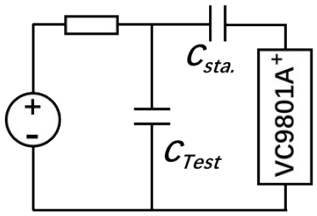

Fig. S12. The circuit connection to test the real capacitance of different kinds of capacitors under different voltage.

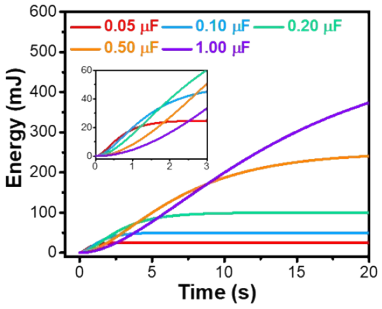

Fig. S13. The energy curves of different capacitance charged by a constant voltage source.

Time (s)	Voltage (V)	Energy (J)	Power (W)					
			Discharge to 0	Discharge to t_1	Discharge to t_2	.....	Discharge to t_n	Discharge to t_{n+1}
0	0	0						
t_1	V_1	E_1	$(E_1-0)/(t_1-0)$					
t_2	V_2	E_2	$(E_2-0)/(t_2-0)$	$(E_2-E_1)/(t_2-t_1)$				
t_3	V_3	E_3	$(E_3-0)/(t_3-0)$	$(E_3-E_1)/(t_3-t_1)$	$(E_3-E_2)/(t_3-t_2)$			
.....	.....	.....	.....	.....	.....	.....		
t_n	V_n	E_n	$(E_n-0)/(t_n-0)$	$(E_n-E_1)/(t_n-t_1)$	$(E_n-E_2)/(t_n-t_2)$	.....		
t_{n+1}	V_{n+1}	E_{n+1}	$(E_{n+1}-0)/(t_{n+1}-0)$	$(E_{n+1}-E_1)/(t_{n+1}-t_1)$	$(E_{n+1}-E_2)/(t_{n+1}-t_2)$	.....	$(E_{n+1}-E_n)/(t_{n+1}-t_n)$	
t_{n+2}	V_{n+2}	E_{n+2}	$(E_{n+2}-0)/(t_{n+2}-0)$	$(E_{n+2}-E_1)/(t_{n+2}-t_1)$	$(E_{n+2}-E_2)/(t_{n+2}-t_2)$	.....	$(E_{n+2}-E_n)/(t_{n+2}-t_n)$	$(E_{n+2}-E_{n+1})/(t_{n+2}-t_{n+1})$
Find maximum power (W)			$P_{max}(D-0)$	$P_{max}(D-t_1)$	$P_{max}(D-t_2)$	.....	$P_{max}(D-t_n)$	$P_{max}(D-t_{n+1})$
			P_{max}					

Fig. S14. Logic diagram to obtain the maximum power of TENG under a capacitance load.

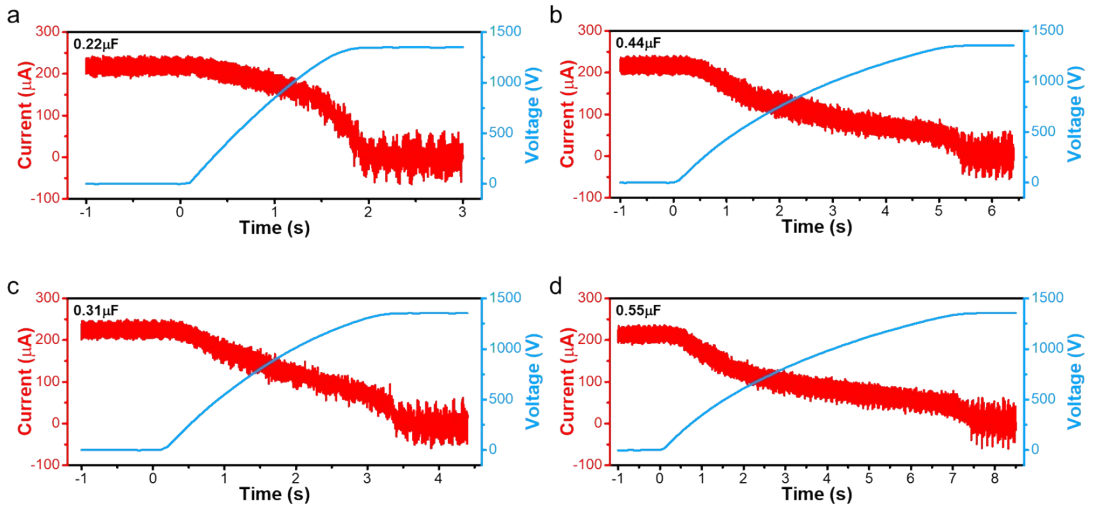

Fig. S15. The voltage of capacitor and output current of TENG changes versus time in the process of TENG charging capacitor under the mechanical input of 4 Hz. The dynamic process of CV-TENG charging a capacitor of (a) 0.22 μF, (b) 0.31 μF, (c) 0.44 μF, and (d) 0.55 μF.

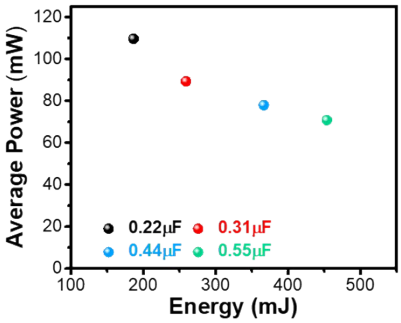

Fig. S16. The relationship between the stored energy of the capacitor and its max average power.

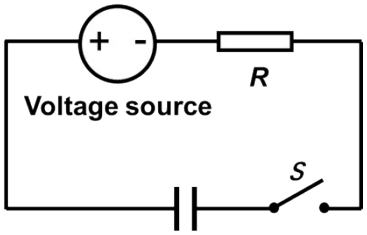

Fig. S17. The circuit connection of the voltage source charging a capacitor.

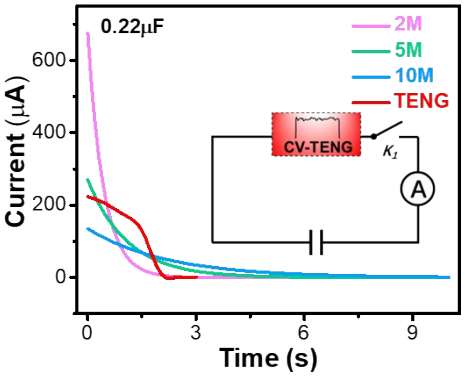

Fig. S18. The current curves change under voltage source with different internal resistance and CV-TENG, respectively.

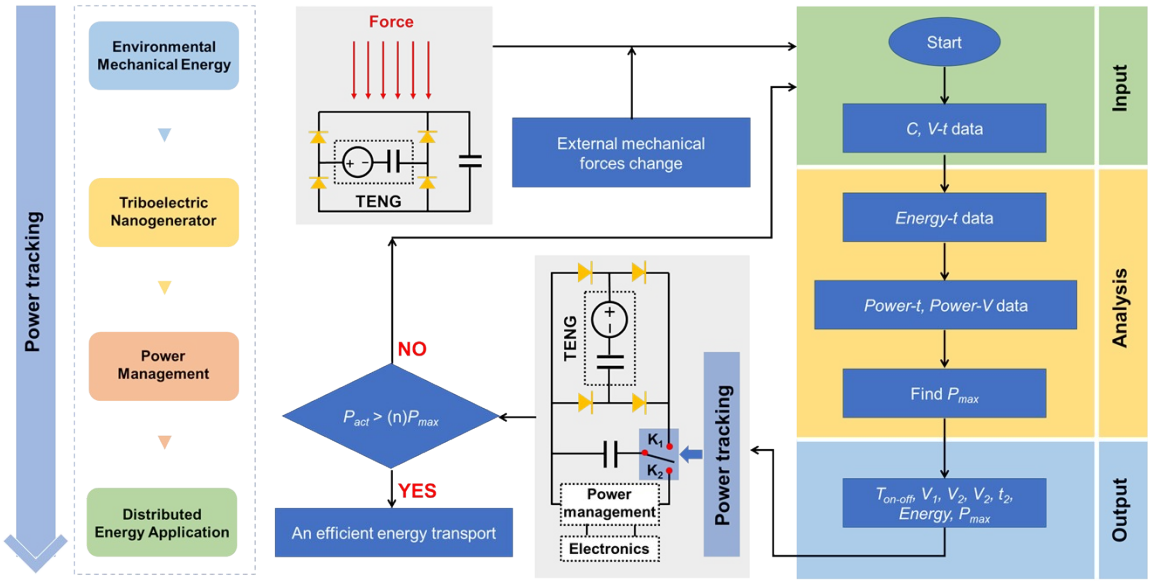

Fig. S19. Logic diagram of energy optimization scheduling.

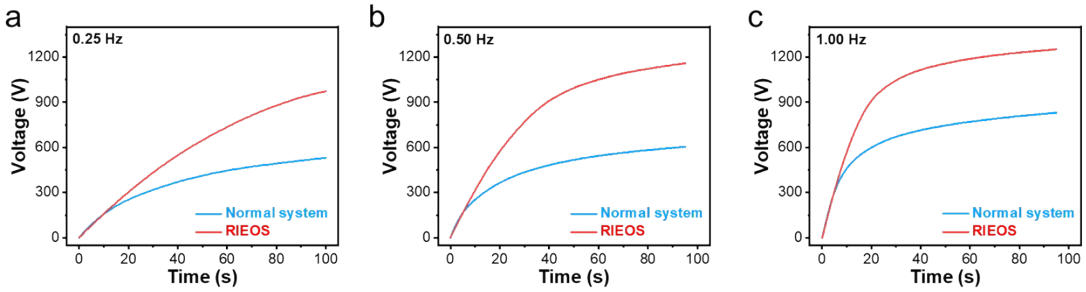

Fig. S20. The voltage curves of RIEOS and normal system under different frequency (a) 0.25 Hz, (b) 0.50 Hz, (c) 1.00 Hz.

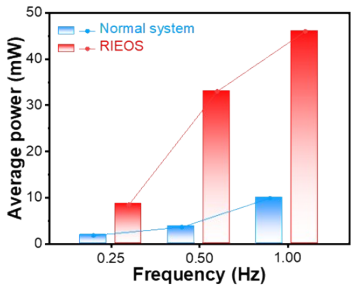

Fig. S21. The average power of RIEOS and normal system in different frequency, respectively.

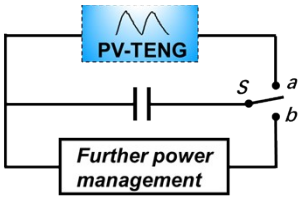

Fig. S22. The general power management strategy of PV-TENG.

	TENG type	Capacitor response	Power management strategy	Environmental monitoring
RIEOS	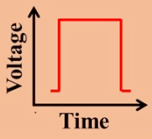		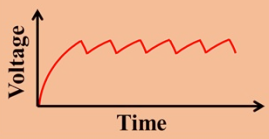	YES
Normal system	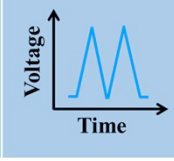	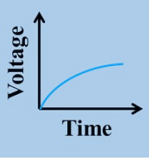	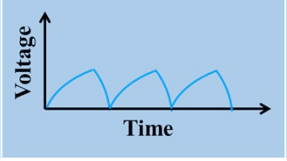	NO

Fig. S23. The difference between RIEOS and the normal system.

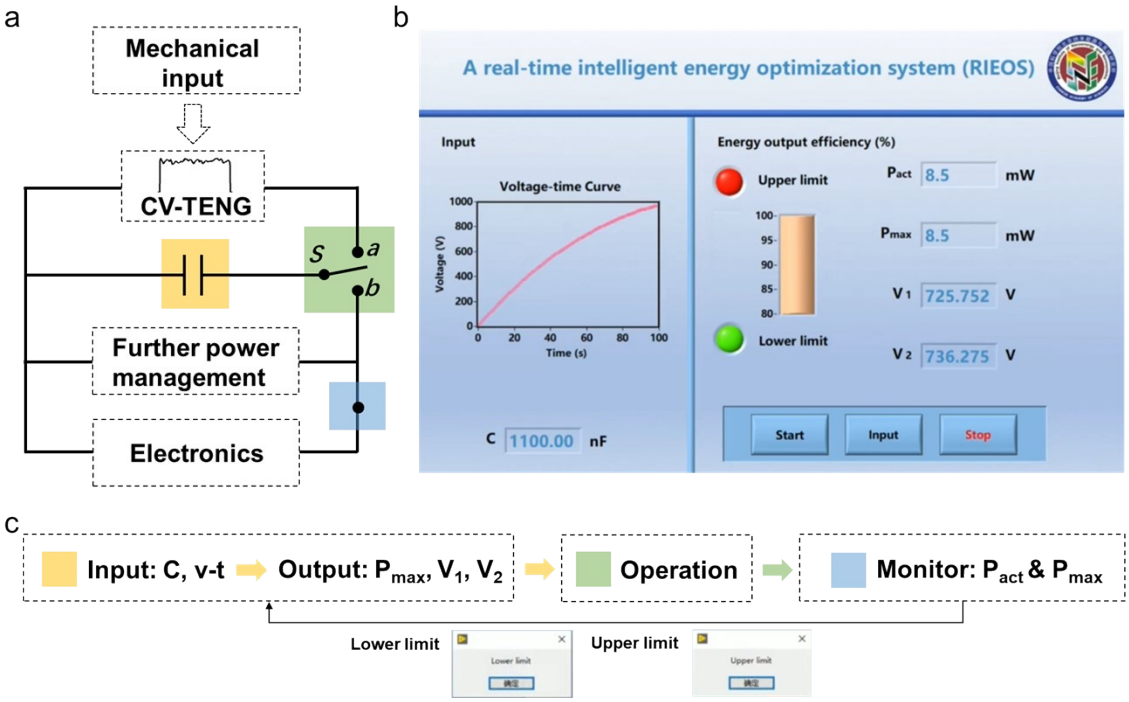

Fig. S24. The detailed explanation about the graphical user interface of RIEOS. (a) The simple schematic diagram of the RIEOS based on Key Node. (b) the graphical user interface of RIEOS. (c) the simple flow map of Key Nodes work.

Supplemental Tables:

Table S1. The capacitance, withstand voltage and category of capacitors.

Type	Capacitance	Withstand Voltage	Category
i	1.1μF	900 V	Thin-film capacitor
ii	1.1μF	2000 V	Ceramic capacitor
iii	1.1μF	900 V	Electrolytic capacitor

Table S2. the U_c changes with time when the capacitor is charged and discharged.

Time	$e^{-t/\tau}$	(U_c) Discharging process
0	e^0=1	U_S
τ	e^{-1}=0.368	$0.368U_S$
2τ	e^{-2}=0.135	$0.135U_S$
3τ	e^{-3}=0.050	$0.050U_S$
4τ	e^{-3}=0.018	$0.018U_S$
5τ	e^{-5}=0.007	$0.007U_S$
∞	$e^{-\infty}$=0	0

Supplemental Notes:

Note S1. The electrical model of TENG in free-standing mode.

Usually, the fundamental working mechanism of the TENG can be regard as a conjugation of contact electrification and electrostatic induction according to the previous theoretical works about TENG. Since the intrinsic device based on electrostatics is a capacitor, TENG will have an inherent capacitive behavior basically. For any TENGs, the governing equation can be given as follows.[1]

$$V = -\frac{1}{C(x)}Q + V_{OC}(x) \qquad (1)$$

where V is the total voltage difference between the two electrodes, C and Q represent the capacitance between the two electrodes and the already transferred charges, V_{OC} is the open circuit voltage between the two electrodes. From this governing equation, the lumped equivalent circuit model can be derived and represented by a serial connection of an ideal voltage source and a capacitor. Considering the inherent capacitance of TENG in free-standing mode is invariable, its lumped equivalent circuit model can be regard as a serial connection of an ideal voltage source and a resister. It can be noted that the inherent impedance of TENG mainly comes from its inherent capacitance.

Note S2. The structure difference between CV-TENG and PV-TENG.

It is worthy to investigate the voltage shape of TENG due to taking dynamic energy transport process as background for obtaining a higher energy output. Figure 2a-2j show the performance of constant/pulse-voltage sources under a capacitance load. It is necessary to carry out experimental verification by CV-TENG and PV-TENG. Here, a conventional pulse-voltage TENG (PV-TENG) with rotational free-standing mode and a constant-voltage TENG (CV-TENG) based on phase-shift design are fabricated to explore the maximum average power of TENG under a capacitance load. As shown in figure S5a and S5b, conventional free-standing mode TENG has two parts, a stator and a rotor, respectively. The stator is a disc with twelve radial and regularly arrayed electrode sectors. The rotor is another disc with six radial arrayed trenches, where dielectric layers are inserted in the trenches. The rotor and stator are stacked in the vertical direction in coaxial

alignment with adaptable contact design, where the gap distance is about 1.0 cm. Based on Kirchhoff's law and the linear circuit superposition principle, the voltage of TENG can be adjusted by changing the position of the trenches on the rotor via phase-shift design as shown in figure S5c. Regular radial arrayed trenches on the rotor make it generates the same pulse-voltage output as conventional TENG. Irregular radial arrayed trenches on the rotor based on phase-shift design make it generates the constant-voltage output, called constant-voltage TENG (CV-TENG), where the dislocation angle of 5° (60° - 55° = 5°) is selected due to the optimization methods in our previous reports.[2, 3] Detailed circuit connection on the stator of the TENG is shown in figure S6, where every two adjacent electrodes constitute a TENG unit, which is connected to a rectifier and then connected in parallel.

Note S3. The output performance comparation between CV-TENG and PV-TENG.

The voltage output of pulse-voltage TENG (PV-TENG) and CV-TENG are shown in figure S7a and S7b. The peak voltage of PV-TENG and the constant-voltage of CV-TENG are both stabilized at ~1400 V under different frequencies, which is consistent with previous reports.[3] It is reasonable that the peak value of PV-TENG and CV-TENG remains the same based on Kirchhoff's law and the linear circuit superposition principle as shown in figure S8. Their average short-circuit current is basically the same at different frequencies (figure S9a). However, the crest factor of CV-TENG is always lower than that of PV-TENG, which is as low as 1.05 at 4 Hz (figure S9b). Meanwhile, CV-TENG and PV-TENG exhibit different charging characteristic under the same capacitance load. The voltage curves and the circuit connection are observed in figure S10a and its inset. At $t = 0$, the capacitance load has been charging at a maximum speed. It is obvious that CV-TENG and PV-TENG has the same average short-circuit current. Although both the charging rate gradually slows down when charging behavior happens, CV-TENG always has a higher instantaneous charging rate than PV-TENG under the same mechanical input of 0.25 Hz. The voltage of capacitor gradually increases to 973.35 V and 530.09 V charged by CV-TENG and PV-TENG in 25 cycles, respectively. During this process, CV-TENG stores the energy of 104.21 mJ, far more than PV-TENG of 30.91 mJ (figure S10b). The energy ratio between CV-TENG and PV-TENG gradually increases up to 3.4 times along the cycles (figure

S10c). The amount of charge and the stored energy transport to the capacitor per cycle changes versus cycles charged by CV-TENG and PV-TENG is exhibited in figure S10d and S10e under the same mechanical input of 0.25 Hz, respectively. CV-TENG exhibits excellent superiority in transferring charges to the capacitor that the charge flowing to the capacitor per cycle is higher than PV-TENG and the stored charges is promoted over 1.55-fold than PV-TENG just in 25 cycles. Similar with electric quantity increasing, the energy output of CV-TENG under a capacitance load is also elevated obviously. The energy transporting to the capacitor per cycle exhibits the unique benefit of CV-TENG in terms of energy output, which is even over 6 times than PV-TENG at the same 18th cycle (figure S10e). Generally, periodic high peak power of TENG has been attracted in some applications due to their high pulse-voltage are easily acquired.[4] There is another method to obtain stable high peak power by adopting the circuit connection in the inset of figure S10f. When switch K_1 or K_2 turns on and switch K_3 points to node a, CV-TENG or PV-TENG starts charging the capacitor. Turn off K_1 and K_2 and switch K_3 points to node b, an instantaneous power (P_{ins}), which could be regard as the peak power, can be generated. In fact, it can be regarded as a RC-circuit in the process of generating instantaneous power, where the transient process experiences 5 τ. The whole derivation is discussed in Note S3. The peak value of instantaneous power depends on two parameters, the triggered voltage and the resistance value of resistor. CV-TENG can generate instantaneous power of 947.43 W when resistor is 100 Ω, it can reach a higher value when increasing the voltage or decreasing the resistance value of resistor (figure S11). It is obvious that the output voltage of TENG and the resistance value of resistor determines the peak value of instantaneous power. As a distributed power source, it is significant to evaluate average power than instantaneous power.[5, 6] The maximum average power output of PV-TENG and CV-TENG can be performed sustainability by discharging at their matched triggered voltage in different charging cycles respectively as shown in figure S10g. Moreover, the energy output of CV-TENG and PV-TENG under a capacitance load in different frequencies is also exhibited in figure S10h. CV-TENG obtains energy output of 104.21, 107.69, 120.43, and 175.39 mJ under 0.25, 1, 2, and 4 Hz in the same cycles, respectively, while PV-TENG only acquires energy output of 30.91, 45.04, 82.09, and 113.35 mJ, respectively. As the frequency increases, the negative effect of pulse-voltage gradually weakens in terms of

energy output. However. CV-TENG can get higher energy output than that of PV-TENG at all different frequencies under a capacitance load. Energy output of CV-TENG even promotes 3.4-fold than PV-TENG in low frequency mechanical energy input (0.25 Hz) in 25 cycles, exhibiting CV-TENG unique advantage in terms of harvesting low frequency mechanical energy efficiently.

Note S4. Instantaneous power of TENGs in circuit connection of Inset of figure S11a.

As shown in the inset of figure S10a, when switch K_1 and K_2 are on and switch K_3 points to Node a, the electric quantity (Q) of the capacitor charged by CV-TENG or PV-TENG can be represented as follows:

$$Q = CU_c \qquad (2)$$

When the capacitor is charged to a saturation voltage (U_S), switch K_3 points from Node a to Node b. At this point, the *RC* circuit is disconnected from the power supply, and the capacitor *C* discharges the resistor *R*. When the switch K_3 is switched from Node a to Node b, according to the circuit change rule, the voltage of the capacitor remains the value of the moment before the circuit change. Then the capacitor starts to discharge, and the voltage of the capacitor decreases from the value of U_c. In the process of capacitor discharge, the charge stored on the capacitor plate decreases continuously, and the discharge current *I* in the circuit also decreases with the decrease of voltage. Finally, the charge stored in the capacitor is exhausted, the capacitor voltage is zero, and the circuit current I is also zero. At this time, the circuit reaches a new steady state, $U_c = 0$, $I = 0$.

In the transient process in which the voltage of the capacitor is zero immediately after the switch *K*3 is switched from Node a to Node b, the voltage equation for the circuit can be listed as follows according to Kirchhoff voltage law (KVL):

$$U_C + IR = 0 \qquad (3)$$

Substitute Equation (1) into the current definition of the capacitor as follows:

$$I = \frac{dQ}{dt} = \frac{CdU_c}{dt} \qquad (4)$$

Equation (2) is obtained when the reference directions of U_C and i are consistent. It shows that the capacitor current is proportional to the change rate of the capacitor applied voltage. The voltage of the capacitor is the same as the voltage of the resistor in the whole process.

$$U_c = -U_R = -IR = -RC\frac{dU_c}{dt} \qquad (5)$$

Apply the transformation to Equation (3) as follows:

$$\frac{dU_C}{dt} + \frac{U_C}{RC} = 0 \qquad (6)$$

Equation (4) is a first-order linear differential equation with constant coefficients, it could be solved to obtain the variation rule of capacitor voltage as follows:

$$U = U_0 * e^{-t/RC} \qquad (7)$$

The changing law of circuit current is as follows:

$$I = \frac{U}{R} = \frac{U_0 * e^{-t/RC}}{R} \qquad (8)$$

And then the time constant τ is introduced:

$$\tau = RC \qquad (9)$$

The time constant determines the speed of discharging process. Theoretically, according to the exponential law of capacitor discharging process, must go through an infinite time, transient process to end, and enter a new stable state. But when the transient process experiences (3~5) τ, the terminal voltage of capacitor has reached 0.7% ~ 5% of the initial voltage, so (3~5) τ is used as the transient process experience time. The table S2 lists the U_c changes with time when the capacitor is charged and discharged.

Therefore, when the electric quantity (Q) of the capacitor is consumed by the resistor, consider the discharging process takes 5τ. The instantaneous power P_{ins} changes as follows:

$$P_{ins} = \frac{0.5CU_s^2}{5\tau} = \frac{0.1 * U_s^2}{R} \qquad (10)$$

Note S5. The derivation formula of average power under a capacitance load.

In view of the average power is an effective and equitable way to evaluate the energy output. The average power of the voltage source under a capacitance load can be derived as follows:

$$P_{ins}^{C} = U_C i = C U_C \frac{dU_C}{dt} \quad (11)$$

$$E_{ins}^{C} = \int_0^T P_{ins}^{C} dt = \int_0^T C U_C \frac{dU_C}{dt} dt = 0.5 C {U_C}^2 \quad (12)$$

$$P_{AP}^{C} = \frac{E_{ins}^{C}}{t} = \frac{C {U_C}^2}{2t} \quad (13)$$

where P_{ins}^{C} is the instantaneous power, E_{ins}^{C} is the instantaneous energy, P_{AP}^{C} is the average power that the voltage source flow to the capacitor, C is the capacitance of capacitor, U_C represents the voltage of capacitor, i is the instantaneous current and t is the charging time.

Generally, the instantaneous power (P_{ins}^{C}), instantaneous energy (E_{ins}^{C}), and average power (P_{AP}^{C}) of a capacitor can be represented using the following equations:[7]

$$P_{ins}^{C} = U_C i = C U_C \frac{dU_C}{dt} \quad (14)$$

$$E_{ins}^{C} = \int_0^T P_{ins}^{C} dt = \int_0^T C U_C \frac{dU_C}{dt} dt = 0.5 C {U_C}^2 \quad (15)$$

$$P_{AP}^{C} = \frac{E_{ins}^{C}}{T} = \frac{C {U_C}^2}{2T} \quad (16)$$

where C is the capacitance of capacitor, U_C represents the voltage of capacitor and T is charging time. In our previous work, the triggering switch was proposed to control the capacitor voltage to prevent from falling to zero, so as to further increase the average power and increase the energy-output efficiency under a capacitance load.

$$P_{AP(new)}^{C} = \frac{E_{ins(T_1)}^{C} - E_{ins(T_2)}^{C}}{T_1 - T_2} = \frac{C\left[U_{C(T_1)}{}^2 - U_{C(T_2)}{}^2\right]}{2(T_1 - T_2)} \quad (17)$$

Where T_1 and T_2 are the corresponding time before and after the switch is triggered. $P_{AP(new)}^{C}$ is the new calculating method of average power for TENG at capacitance load. The energy increment and charge increment of capacitor are respectively as follows:

$$\Delta E_C = 0.5C\left[U_{C(T_1)} + \left(U_{C(T_2)} - U_{C(T_1)}\right)e^{-t/RC}\right]^2 - 0.5CU_{C(T_2)}^2 \quad (18)$$

$$\Delta q = q(T_1) - q(T_2) = C\left[U_{C(T_1)} + \left(U_{C(T_2)} - U_{C(T_1)}\right)e^{-t/RC}\right] - CU_{C(T_2)} \quad (19)$$

The incremental electric energy from the power source is as follows:

$$\Delta E = U \times \Delta q = U_{C(T_1)}C\left(U_{C(T_1)} - U_{C(T_2)}\right)(1 - e^{-t/RC}) \quad (20)$$

Where *R* is the inherent resistance of CV-TENG.[3]

Note S6. The charging process of RC circuit.

As shown in the inset of figure S16, define the voltage of constant voltage source is *E*, the resistance and the capacitor in the circuit are *R* and *C*, respectively. the voltage of resister is U_R, and the voltage of capacitor is U_C. When the switch S is not closed, there is no voltage at both ends of the capacitor, that is, U_C is equal to 0, and the current (*i*) in the circuit is 0. In the transient process from the moment the switch S is closed to the capacitor voltage is U_C, the following equation can be listed for the circuit according to Kirchhoff's law：

$$E = U_R + U_C = iR + U_C \quad (21)$$

The charge stored in capacitor is given by the following equation：

$$Q = CU_C \quad (22)$$

Substitute Equation (10) into the current definition of capacitor as follows：

$$i = \frac{dq}{dt} = \frac{d(CU_C)}{dt} = C\frac{dU_C}{dt} \quad (23)$$

Equation (11) is obtained when the reference directions of U_C and i are consistent. It shows that the capacitor current is proportional to the change rate of the capacitor applied voltage.

Substitute Equation (11) into Equation (9) as follows：

$$RC\frac{dU_C}{dt} + U_C = E \quad (24)$$

Equation (12) is a first-order linear differential equation with constant coefficients, it could be solved to obtain the variation rule of capacitor voltage as follows:

$$U_C = E - E \cdot e^{-\frac{t}{RC}} = E\left(1 - e^{-\frac{t}{RC}}\right) \quad (25)$$

Note S7. The difference between RIEOS and the normal system.

Generally, due to TENG's output characteristics of low current, high voltage and huge internal impedance difference with the electronics, there are great challenges for connecting TENGs and the electronics with efficient combination. Previous studies have introduced the power management to achieve the function of boosting the current and lowering the voltage, helping the electricity generated by TENGs to transport the energy to the electronics. However, it is difficult to obtain maximum energy output of the PV-TENG in power management strategy. As shown in figure S22, it is the general power management strategy of PV-TENG.[8, 9] Similar to CV-TENG, it also needs to charge the capacitor and then release the stored energy at the right voltage. In general, a proper voltage is selected to discharge in capacitor based on circuit management of PV-TENG, but whether the maximum energy output is reached is not discussed. In this work, the difference between RIEOS and the normal system is shown in figure S23. The normal system consists of three common components: a conventional PV-TENG, a normal capacitor, and a general power management strategy that releases energy at 300 V. While, the RIEOS consists of three complementary components: a CV-TENG, a thin-film

capacitor, and a power management control module that releases energy at optimal voltage to maintain efficient energy transmission and cope with unstable environmental input. Therefore, the RIEOS maintains the efficient electricity supply and transmission implemented at every node and link in energy transport.

Note S8. The description of Video S1 corresponding to RIEOS.

The Video S1 shows a brief description of how RIEOS works under changes in wind speed. First, the wind speed is 0.25 Hz, the voltage-time curve is collected by the RIEOS to obtain the V_1, V_2 *and* P_{max}, the RIEOS regulates the power management module based on these values and monitors the P_{act}. Taking into account power losses, the P_{act} is generally less than the P_{max}. (Here we set the transmission efficiency of 80%, which can be changed according to the actual circuit situation.) At this time, all RIEOS modules maintain efficient energy transport. Since the power management module at this time is based on the analysis of the voltage-time curve when the wind speed is 0.25Hz, if the wind speed changes without adjusting the power management module parameters, it will not be able to guarantee the efficient energy transport after the wind speed changes. This is also a thorny problem that most conventional power management cannot solve. The RIEOS provides a monitor module, it can determine whether the wind speed has changed by the ratio of the two (P_{act} *and* P_{max}). If the wind speed changes, RIEOS will alarm (Upper limit or Lower limit) and re-enter the voltage-time curve to obtain the best power management parameters after the wind speed change, and maintain the efficient energy transport.

Note S9. The detailed explanation about the graphical user interface of RIEOS.

Here, the detailed explanation about the graphical user interface of RIEOS is exhibited as shown in figure S24. Figure S24a is a simple schematic diagram of the RIEOS based on Key Node. The Yellow Key Node is the capacitance load of CV-TENG. It is responsible for taking the voltage-time curve of the capacitor and entering it into the RIEOS system to obtain the V_1, V_2, and maximum energy power (P_{max}), and transmitting it to the Green Key Node to run the power management module according to this result. Meanwhile, Blue Key

Node is a monitor that get the actual power (P_{act}) of RIEOS and compare it with the P_{max}. Taking into account power losses, the P_{act} is generally less than the P_{max}. (Here we set the transmission efficiency of 80%, which can be changed according to the actual circuit situation.) But if the mechanical input changes, the ratio between the two will not be between 80% and 100%. If the mechanical input is smaller, P_{max} will be much smaller than P_{act}, which will show the "Lower limit", and if the mechanical input is larger, P_{max} will be much larger than P_{act}, which will show the "Upper limit". At this point, RIEOS will alert, the Yellow Key Node will re-enter the voltage-time value to ensure efficient energy transfer even if the mechanical input changes. Figure S24b is the graphical user interface of RIEOS, the Start and Stop buttons are used to start and shut down the RIEOS. The Input button is used to access the voltage-time curve in the initial startup state, and the late voltage-time curve is automatically connected when the limit is exceeded. Figure S24c is a simple flow map of Key Nodes work. Three Key Nodes represent input & output, operation, and monitor responsibilities to ensure efficient energy transport throughout RIEOS.

Supplemental videos:

Video S1. The show of the software interface when calculating different frequencies.

Methods

Fabrication and electrical measurement of the triboelectric nanogenerator

Rotor: (1) Cut a disc-shaped acrylic sheet as a substrate with a radius of 15 cm by 3mm using a laser cutter; (2) Create radial-arrayed trenches which define the location of dielectric layer on the substrate using laser cutting; (3) Paste the dielectric layer in the trenches; (4) Drill through-holes on center of the substrate for mounting it on a mechanical stage by screws. Stator: (1) Cut a disc-shaped sheet as a substrate with a radius of 15 cm; (2) Plate a layer of Cu (1.6 mm) as electrode with the PCB technology. (3) Connecting every two electrodes to rectifier and parallel them. This fabrication method is following the article of *Energy Environ. Sci.*,2022, 15, 1334 (A highly efficient constant-voltage triboelectric nanogenerator).

Experimental setup for electric measurement

(1) Mount a rotary motor in an inverted way on a working stage; (2) Insert the shaft on the motor into the central hole of the rotor; (3) Align the rotor and the stator to make them in coaxial alignment; (4) Adjust height so that the dielectric layer on the rotor and the stator are in contact.

Electrical measurement

The programmable electrometer (Keithley model-6514) was adopted to test the current output of TENG at resistance load. A mixed domain oscilloscope (MDO3024, the attenuation coefficient of the high voltage probe is 1000 times, and the circuit input impedance is 100M) was used to test the open-circuit voltage of the TENG. An electrostatic voltmeter (Trek Model-347) was used to test the voltage curve of the capacitor. Electrical theory data from LTspice.

References

1 S. Niu, S. Wang, L. Lin, Y. Liu, Y. Zhou, Y. Hu, and Z. L. Wang, *Energy Environ. Sci.*, 2013, **6**, 3576-3583.

2 X. Li, X. Yin, Z. Zhao, L. Zhou, D. Liu, C. Zhang, C. Zhang, W. Zhang, S. Li, J. Wang, and Z. L. Wang, *Adv. Energy Mater.*, 2020, **10**, 1903024.

3 X. Li, C. Zhang, Y. Gao, Z. Zhao, Y. Hu, O. Yang, L. Liu, L. Zhou, J. Wang, and Z. L. Wang, *Energy Environ. Sci.*, 2022, **15**, 1334-1345.

4 Z. Wang, W. Liu, W. He, H. Guo, L. Long, Y. Xi, X. Wang, A. Liu, and C. Hu, *Joule*, 2021, **5**, 441-455.

5 Z. Cao, Z. Wu, R. Ding, S. Wang, Y. Chu, J. Xu, J. Teng, and X. Ye, *Nano Energy*, 2022, **93**, 106891.

6 Y. Gao, D. Liu, Y. Li, J. Liu, L. Zhou, X. Li, Z. Zhao, S. Li, P. Yang, Z. L. Wang, and J. Wang, *Energy Environ. Sci.*, 2023, **16**, 2304-2315.

7 S. Niu, Y. Liu, Y. Zhou, S. Wang, L. Lin, and Z. L. Wang, *IEEE T. electron dev.*, 2015, **62**, 641-647.

8 X. Cheng, W. Tang, Y. Song, H. Chen, H. Zhang, and Z. L. Wang, *Nano Energy*, 2019, **61**, 517-532.

9 W. Harmon, D. Bamgboje, H. Guo, T. Hu, and Z. L. Wang, *Nano Energy*, 2020, **71**, 104642.